Monthly Notices
of the
ROYAL ASTRONOMICAL SOCIETY

MNRAS **485,** 4128–4133 (2019)
Advance Access publication 2019 March 11

doi:10.1093/mnras/stz707

# Constant light element abundances suggest that the extended P1 in NGC 2808 is not a consequence of CNO-cycle nucleosynthesis

I. Cabrera-Ziri [1]★† C. Lardo [2] and A. Mucciarelli[3,4]

[1]*Harvard–Smithsonian Center for Astrophysics, 60 Garden Street, Cambridge, MA 02138, USA*
[2]*Laboratoire d'Astrophysique, Ecole Polytechnique Fédérale de Lausanne, Observatoire de Sauverny, CH-1290 Versoix, Switzerland*
[3]*Dipartimento di Fisica e Astronomia, Università degli Studi di Bologna, via Piero Gobetti 93/2, I-40129, Bologna, Italy*
[4]*INAF-Astrophysics and Space Science Observatory Bologna, via Piero Gobetti 93/3, I-40129, Bologna, Italy*

Accepted 2019 March 7. Received 2019 February 17; in original form 2018 November 8

## ABSTRACT

Recent photometric results have identified a new population among globular cluster stars. This population, referred to as the 'extended P1', has been suggested to be the manifestation of a new abundance pattern where the initial mass fraction of He changes among cluster stars that share the same CNO values. The current paradigm for the formation of the multiple stellar populations in globular clusters assumes that variations in He are the product of chemical 'enrichment' by the ashes of the CNO-cycle (which changes He and other elements like C, N and O simultaneously). We obtained MIKE@Magellan spectra of six giant stars in NGC 2808, a cluster with one of the strongest examples of the extended P1 population. We provide the first complete characterization of the light elements abundances for the stars along a significant range of the extended P1 photometric group. The stars from our sample appear to be homogeneous in C, N, O, Na, Mg and Al. The lack of a significant change in these products of the CNO-cycle suggests that unlike the rest of the populations identified to date, the photometric changes responsible for the extended P1 feature are a consequence of an alternative mechanism. Our measurements are consistent with the interpretations where the changes of the He mass fraction among these stars could be a consequence of p–p chain nucleosynthesis (which could increase the He in stars without affecting heavier elements). Having said that, direct measurements of He are necessary to conclude if variations of this element are present among extended P1 stars.

**Key words:** stars: abundances – globular clusters: general – globular clusters: individual: NGC 2808.

## 1 INTRODUCTION

It is a well-established fact that globular clusters host multiple stellar populations with different abundance variations of specific light elements. These variations are not random but instead follow distinct correlation patterns between different elements (cf. Charbonnel 2016; Bastian & Lardo 2018, for recent reviews). Evidence for the multiple stellar populations has been detected in clusters spanning a large range of metallicities, masses, ages and galactic environments (e.g. Larsen et al. 2014; Milone et al. 2017; Niederhofer et al. 2017; Schiavon et al. 2017b; Martocchia et al. 2018).

For decades it has been known that populations of stars with different light elements abundances occupate different regions of the colour–magnitude diagram in a given evolutionary stage (e.g. Bond & Neff 1969; Osborn 1976; Marino et al. 2008). Today we can identify distinct sub-populations with extreme efficacy when precise abundances and ultraviolet photometry are combined (e.g. Milone et al. 2015b; Carretta et al. 2018).

Milone et al. (2015a) introduced a pseudo colour–colour plot (a.k.a. chromosome map) using F275W, F336W, F438W and F814W *HST* filters that allow a clear distinction between photometric sub-populations (e.g. bottom panel of Fig. 1). These photometric sub-populations have different abundances of light elements like Na, Mg and Al (e.g. Carretta et al. 2018); however, these broad-band photometric filters are not sensitive to changes in the abundances of these particular elements but are sensitive to C, N, O and He instead (Sbordone et al. 2011).

Recent work has focused on the interpretation of the chromosome map with the main goal of identifying what drives the position of the stars in this plane. The approach has been to compute stellar atmospheres with different stellar parameters and relative abundances between elements, then synthesize the photometry for

★ E-mail: ivan.cabrera@cfa.harvard.edu
† Hubble fellow.

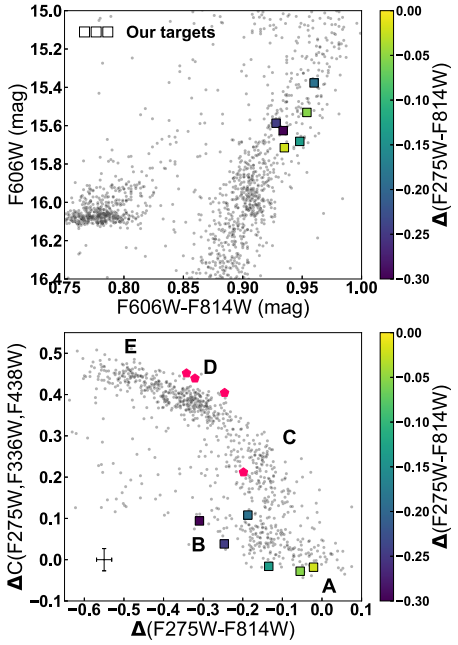


**Figure 1.** Squares represent the stars in our spectroscopic study while the small dots other NGC 2808 stars. Upper panel: position of our targets in the optical CMD. Lower panel: Chromosome map of NGC 2808 RGB stars. Colour coded is the position of the stars in our sample in the horizontal axis of the chromosome map. The letters show the general position of the five populations identified by Milone et al. (2015b): A and B with field like N (i.e. P1) while B, C and D with enhanced N with respect of field stars (i.e. P2). Our sample is distributed along the entire P1, sampling both population A and B. The pink pentagons show P2 stars with archival GIRAFFE, we show them here and in Fig. 2 to illustrate how these populations map from photometric to abundance space (no match found between UVES data and stars in the Lardo et al. chromosome map). The error bars represent the mean uncertainties of all the data points in the lower panel.

each case and see where it lies in the chromosome map (e.g. Lardo et al. 2018; Milone et al. 2018). There is a general consensus among these studies in that vertical changes in the chromosome map are mostly due to N variations while horizontal changes respond to variations in temperature, a consequence of different He mass fractions of the stars.[1]

With this knowledge in hand, it is possible to identify a population in the chromosome maps of several clusters that would have significant changes in He at a constant N abundance consistent with field stars (cf. Milone et al. 2017). From now on we will refer to this population as extended P1 (P1 being the population in globular clusters with N abundance akin to field stars of similar [Fe/H].). The extended P1 cannot be accounted for by photometric uncertainties alone, for example, the difference between the most extreme stars in population A and B is >15 times the size of the mean photometric uncertainties (cf. Fig. 1), suggesting that its presence reflects genuine He abundance variations among these stars (cf. Lardo et al. 2018). If this interpretation were to be correct, this population would have a deep impact on our understanding of the origin of the abundance variations characteristic of globular clusters, as it would be a chemical pattern very difficult to account for with the current models (cf. Lardo et al. 2018, more on this in Sections 4 and 5).

The broad consensus among these models/scenarios is that nucleosynthesis via the CNO-cycle is responsible for producing He variations and changes in other elements like C, N, O, Na, Mg and Al that have been inferred though photometry and directly measured in spectroscopic campaigns. With the main difference between models being the site where these reactions take place, which include in principle: the core of massive main sequence stars; the H-burning shell in stars at the tip of the RGB and RGB clump; as well as in the bottom of the convective envelope in (super)AGB stars (cf. Charbonnel 2016, and references therein).

During the CNO-cycle, nuclear fusion turns H into He with the help of C, N and O as catalysts (where C and O turn into N, and so changing their relative abundances). If the temperature increases, the NeNa-chain activates with a net result of depleting O while enhancing Na. An additional increase in temperature triggers the MgAl-chain which ends up producing Al and depleting Mg (cf. Cassisi & Salaris 2013; Charbonnel 2016, and references therein). These abundance patterns qualitatively agree with the observed abundance variations among globular cluster stars,[2] as a consequence the origin of the latter was linked to these reactions (cf. Bastian & Lardo 2018).

Milone et al. (2015b) identified five sub-populations in the chromosome map of NGC 2808, two of them (photometric groups A and B) among the extended P1 (cf. Fig. 1). The abundances of several elements have been determined for stars belonging to group B (e.g. Milone et al. 2015b; Carretta et al. 2018). These have been found to be consistent with the values of field stars of similar [Fe/H]; however, the abundance of N has not been investigated.[3] However, the chemical composition of stars from photometric group A has not been measured to date, although they are key to constraining what kind of chemical differences are present within population P1 in the chromosome map.

In this work, we present spectroscopic abundances (including [N/Fe]) of the extended P1 of NGC 2808, a cluster with one of the largest extended P1 in Milone et al. (2017), sampling for the first time stars from groups A and B with the aim of testing the predicted homogeneity in the abundances of CNO-cycle products (e.g. C, N and O) proposed by different interpretations of the chromosome map.

## 2 DATA

The present work is centred in the analysis of high-resolution spectra of six stars, all of them members of NGC 2808 according to proper motions and radial velocities (cf. Table 1). These stars were chosen to occupy very similar regions in the optical CMD in order to minimize effects arising from differences in stellar parameters; however, they stretch along most of P1 extent in the chromosome map, sampling both population A and B defined in Milone et al. (2015b) (cf. Fig. 1). The models of Lardo et al. (2018) suggest that the difference in the He mass fraction between population B and A

[1]For completeness, it has been also pointed out that significant variations in the overall C+N+O, heavy elements and s-process are associated with the horizontal position of the stars in the chromosome maps as well, i.e. type II clusters in Milone et al. (2017).

[2]Although there are some caveats with this picture e.g. Bastian, Cabrera-Ziri & Salaris (2015), Prantzos, Charbonnel & Iliadis (2017), Carretta et al. (2018).

[3]Carretta et al. (2018) reported the relative CN abundance of 89 stars, a rough proxy for N. They found that the CN abundance of group B stars was lower than any of the other groups (excluding group A which was not represented in their sample).

**Table 1.** Radial velocities, stellar parameters and abundances of our targets.

| Star ID* | RV (km s$^{-1}$) | $T_{\rm eff}$ (K) | log(g) (cm s$^{-2}$) | $v_t$ (km s$^{-1}$) | [C/Fe] (dex) | [N/Fe] (dex) | [O/Fe] (dex) | [Na/Fe] (NLTE) (dex) | [Mg/Fe] (dex) | [Al/Fe] (dex) | [Si/Fe] (dex) | [Fe/H] (dex) |
|---|---|---|---|---|---|---|---|---|---|---|---|---|
| 55974[a] | 95.90 ± 0.89 | 4809 | 2.15 | 1.30 | 0.05 ± 0.16 | 0.08 ± 0.17 | 0.37 ± 0.16 | −0.33 ± 0.05 | 0.18 ± 0.06 | −0.04 ± 0.09 | 0.18 ± 0.09 | −1.10 ± 0.09 |
| 57615[a] | 81.08 ± 1.08 | 4796 | 2.08 | 1.30 | −0.20 ± 0.13 | 0.05 ± 0.17 | 0.39 ± 0.13 | −0.51 ± 0.08 | 0.11 ± 0.06 | −0.06 ± 0.11 | 0.17 ± 0.10 | −0.87 ± 0.09 |
| 126605[b] | 86.30 ± 1.10 | 4869 | 2.14 | 1.10 | −0.22 ± 0.13 | 0.13 ± 0.19 | 0.40 ± 0.17 | −0.35 ± 0.05 | 0.10 ± 0.06 | −0.02 ± 0.07 | 0.08 ± 0.08 | −1.08 ± 0.09 |
| 187128[b] | 105.87 ± 1.46 | 4776 | 2.01 | 1.70 | −0.03 ± 0.14 | 0.40 ± 0.19 | 0.35 ± 0.12 | −0.17 ± 0.04 | −** | 0.04 ± 0.08 | 0.15 ± 0.07 | −0.92 ± 0.07 |
| 276739[b] | 118.24 ± 1.40 | 4851 | 2.15 | 1.00 | 0.00 ± 0.16 | −0.04 ± 0.17 | 0.45 ± 0.14 | −0.36 ± 0.06 | 0.07 ± 0.06 | −0.11 ± 0.09 | 0.10 ± 0.09 | −1.04 ± 0.09 |
| 298744[a] | 97.76 ± 1.13 | 4851 | 2.18 | 1.40 | 0.00 ± 0.12 | 0.21 ± 0.17 | 0.49 ± 0.17 | −0.41 ± 0.04 | 0.18 ± 0.04 | −0.07 ± 0.07 | 0.09 ± 0.08 | −0.96 ± 0.08 |
| 34250[d] | 110.37 ± 1.86 | 4490 | 1.50 | 1.57 | – | – | – | 0.04 ± 0.05 | −0.08 ± 0.04 | – | 0.18 ± 0.07 | −1.05 ± 0.06 |
| 127544[d] | 111.88 ± 1.38 | 4437 | 1.41 | 1.38 | – | – | – | 0.07 ± 0.05 | 0.00 ± 0.04 | – | 0.24 ± 0.06 | −1.09 ± 0.06 |
| 184806[c] | 112.13 ± 2.35 | 4725 | 1.87 | 1.04 | – | – | – | −0.20 ± 0.04 | 0.14 ± 0.04 | – | 0.07 ± 0.07 | −0.97 ± 0.06 |
| 257773[d] | 112.37 ± 1.10 | 4486 | 1.49 | 1.49 | – | – | −0.04 ± 0.13 | −0.01 ± 0.05 | 0.06 ± 0.15 | – | 0.17 ± 0.09 | −1.06 ± 0.08 |

*Note*: Typical errors in $T_{\rm eff}$, log(g) and $v_t$ are ±75 K, ±0.2 cm s$^{-2}$ and ±0.2 km s$^{-1}$, respectively.

*The letters next to the ID of the stars represent the photometric group to which they are most likely associated.

**Mg for this star is in the flat part of the curve of growth, hindering a reliable estimate.

is of $\Delta Y \sim 0.06$ (assuming the standard $Y = 0.246$ for population A). The same models also suggest that [N/Fe] should be the same in both populations.

The spectra were taken with MIKE at the Magellan-Clay Telescope (Bernstein et al. 2003) during the nights of 2018 January 15–16, using the 0.7 × 5 arcsec$^2$ slit, providing a spectral resolution of ∼36 000 in the red arm. The data were reduced with the `CarPy` version of the pipeline (Kelson 2003) and corrected for tellurics using the `telluric` task in `IRAF`. In addition to the scientific targets, two spectrophotometric standards (GD 71 and LT 3218) were observed with the 2 × 5 arcsec$^2$ slit to allow a relative flux calibration of the science targets.

The photometry used throughout the paper is from the catalogues published by Soto et al. (2017), and the data for the chromosome maps are from Lardo et al. (2018). Finally, we note that all our stars are consistent with the radial velocities previously reported for cluster members (systemic RV = 101.4 ± 1 km s$^{-1}$ and central radial velocity dispersion $\sigma$ = 18.8 ± 4.0 km s$^{-1}$; cf. Lardo et al. 2015) and proper motions (i.e. all targets with a 0.0 displacement in pixels after ΔEpoch = 7.5 yr, cf. D_x and D_y values in the Soto et al. 2017, catalogues). This implies that these stars are unlikely members of the field.

## 3 ANALYSIS

The atmospheric parameters were determined from the *VI* photometry of our targets. Effective temperature $T_{\rm eff}$ values were obtained from $(V - I_C)$ colours using the Alonso, Arribas & Martínez-Roger (1999, 2001) calibration and adopting a colour excess $E(B - V) = 0.22$. Initial surface gravity (log (g)) values were derived using the standard formula:

$$\log\left(\frac{g}{g_\odot}\right) = 0.4(M_{\rm V} + {\rm BC} - {\rm M_{bol,\odot}}) + 4\log\left(\frac{T_{\rm eff}}{T_{\rm eff,\odot}}\right) + \log\left(\frac{M}{\rm M_\odot}\right)$$

assuming $M_{\rm bol,\odot} = 4.75$, $T_{\rm eff,\odot} = 5777$ K, and $\log(g)_\odot = 4.44$ for the Sun. We adopted a stellar mass of 0.8 $M_\odot$ and calculated the bolometric corrections (BCs) using the calibration given in Alonso et al. (1999). Finally, initial microturbulent velocities ($v_t$) were estimated to be 1.5 km s$^{-1}$ for all stars in our sample. From that initial guess, the final $v_t$ values were obtained by erasing any trend between Fe I and the logarithm of the reduced equivalent widths (log (RW) = log (EW/λ)). We note that the spectroscopic parameters are consistent, within the uncertainties, with the photometric ones and the use of the former does not change the results discussed here.

We determined the chemical abundances for all the studied elements (but C and N) through the measurement of the equivalent widths (EWs) of atomic transition lines and employing the package `GALA` (Mucciarelli et al. 2013) based on the `width9` code by R. L. Kurucz. Model atmospheres were calculated with the `ATLAS9` code assuming local thermodynamic equilibrium (LTE) and one-dimensional, plane-parallel geometry; starting from the alpha enhanced grid of models available in F. Castelli's website (Castelli & Kurucz 2003). For all the models we adopted an input metallicity of [A/H] = −1.15 dex according to the value given in Carretta (2015).

For C and N, we measured the G-band feature at 4300 Å and the CN *UV* feature at ∼3880 Å, respectively. Abundances were measured through a $\chi^2$-minimization between the observed spectrum and a grid of synthetic spectra calculated at different abundances. The synthetic spectra have been computed by means of `SYNTHE` code developed by Kurucz, including the entire Kurucz/Castelli line-list (both for atomic and molecular transitions) and adopting the same model atmospheres used to derive the abundances from EWs.

Corrections for departures from the LTE approximation are applied only for the Na lines by interpolating on the grid of corrections calculated by Lind et al. (2011).[4] Reference solar abundances are from Grevesse & Sauval (1998).

The uncertainties in the chemical abundances were obtained as discussed in e.g. Mucciarelli et al. (2017). For those elements for which abundances have been measured using EWs, the random errors are computed as the dispersion of the mean normalized to the root mean square of the number of used lines. For the elements measured via spectral synthesis, the random error has been estimated using Montecarlo simulations, adding Poissonian noise into the best-fitting spectrum in order to reproduce the measured signal-to-noise ratio and creating for each star a sample of 100 noisy synthetic spectra. These spectra have been re-analysed with the same procedure used for the observed spectra and the 1$\sigma$ dispersion of the abundance distribution taken as uncertainty. Uncertainties in chemical abundances due to the adopted model atmospheres were estimated by varying the stellar parameters, one at a time, in steps equal to the uncertainties in $T_{\rm eff}$, log (g) and $v_t$ respectively (cf. Table 1).

Fig. 2 shows the abundance of the main elements known to change the most from star-to-star in GCs (the main products of hot H-burning). The squares in the figure denote stars in our sample while

[4]From the INSPECT database, version 1.0 http://inspect.coolstars19.com

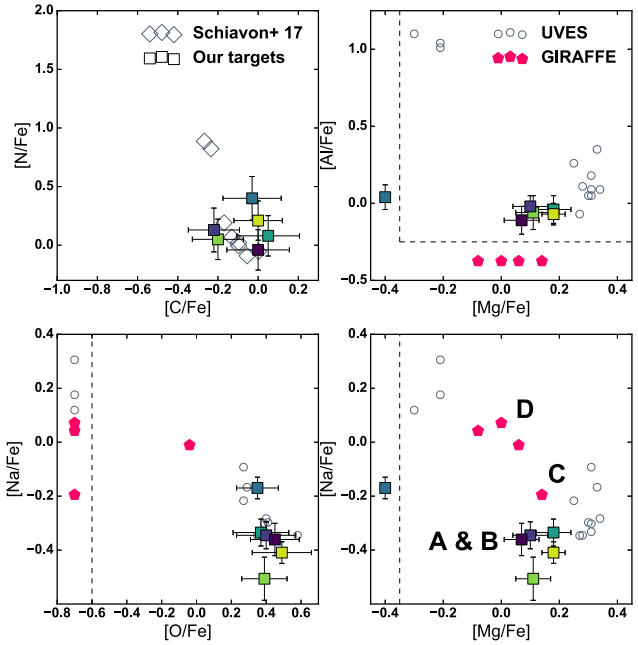


**Figure 2.** Comparison of abundances of our targets stars (square symbols) against reference data (other symbols). The colour of the square symbols represents the Δ(F275W-F814W) value of the P1 stars in our sample (cf. Fig. 1). Upper left*:* N–C abundances of M 107 stars (similar metallicity than NGC 2808) as reference. The other panels display as a reference abundances from archival UVES and GIRAFFE data of NGC 2808. Upper right*:* Al-Mg plane; Lower left (right)*:* Na-O (Na-Mg) plane. The pink symbols are P2 stars in common with Lardo et al. (2018) chromosome map. Stars without [element/Fe] measurements were assigned arbitrary values smaller than the respective dashed line. The letters in the Na-Mg plane denote their positions in the chromosome map from Fig. 1. In none of the cases we find evidence of significant abundance variations among our targets.

the diamonds, circles and pentagons denote reference literature and archival data. For C and N we use the abundances of M 107 (similar [Fe/H] than NGC 2808) from Schiavon et al. (2017a) as reference. For Na, O, Al and Mg we use as a reference abundances derived from UVES- and GIRAFFE-VLT archival data of NGC 2808 stars (programme ID: 072.D-0507). These archival data were analysed in the same way as our extended P1 targets.

## 4 INTERPRETATION

In agreement with previous studies (e.g. Milone et al. 2015b; Carretta et al. 2018), Fig. 2 shows that the abundances of photometric group B are consistent with abundances of field stars with similar [Fe/H], while stars from photometric groups C and D show abundance variations with respect of field stars of similar [Fe/H] (i.e. high Na with low O and Mg). Furthermore, this figure also shows that the stars in our sample from photometric groups A and B in the chromosome maps are homogeneous in the abundances C, N, O, Na, Mg and Al (i.e. both with field like composition).

Changes in the abundance of O, Mg and Si have been suggested to influence where stars lie along the Δ(F275W-F814W) in the chromosome map, namely: changes in O could change the photometry of F275W as a relatively strong OH band falls within the passband of the filter; while changes in Mg and Si could affect the $T_{\rm eff}$ of metal-poor stars (cf. Lardo et al. 2018, and references therein). However, these effects do not seem to be responsible for the Δ(F275W-F814W) positions of the stars in our sample; they all appear to be homogeneous in the abundances of these elements and the largest $T_{\rm eff}$ difference between our stars is only ∼90 K (cf. Table 1 and Fig. 3). No evidence for significant heavy element variations is found in our sample either (cf. Fig. 3). This suggests that the mechanism responsible for the horizontal extent of our stars in the chromosome map is of a different nature than the one affecting the type II clusters described in Milone et al. (2017).

The absence of a significant variation in the abundances of these CNO-cycle products among our sample of P1 stars of different photometric groups suggests that a different mechanism is responsible for these photometric variations. This would be in stark contrast with the current paradigm in which the photometric sub-populations found among globular cluster stars are the consequence of abundance variations produced by CNO-cycle nucleosynthesis (cf. reviews by Gratton, Sneden & Carretta 2004; Gratton, Carretta & Bragaglia 2012; Charbonnel 2016; Bastian & Lardo 2018, and references therein).

An interpretation that would fit the current evidence would be the one proposed by Lardo et al. (2018) and Milone et al. (2018). This is that changes in the temperature among the extended P1 stars are responsible for this photometric signature in the chromosome maps. In this hypothesis, these temperature changes are a consequence of different He mass fractions among the extended P1 stars. However, these works explicitly state that this is premised upon the extended P1 stars being homogeneous in C, N and O. At the time of writing, there is no direct evidence of He variations among the extended P1 stars (e.g. spectroscopic studies of the strength of He lines in P1 stars of different temperature), so they remain conjectures.

### 4.1 Implications of the possible He variations among extended P1 stars

Under the working hypothesis that the results of synthetic spectral models by Lardo et al. (2018) and Milone et al. (2018) are correct, and that changes in Δ(F275W-F814W) reflect the consequences of He variations, we can identify a possible nucleosynthetic channel for its production.

As mentioned above He is the primary product of H-burning, and the current evidence would indicate that at least two different channels are in play during the production of He-rich material found in globular cluster stars: one producing the well-studied He, C, N, O, Na, Mg and Al anticorrelations (akin to the products of nucleosynthesis through the hot CNO-cycle, that would describe P2 stars) and the other producing He variations without any corresponding change to other light elements (similar to the ashes of the proton–proton chain, which would be more appropriate for the evidence from our sample of P1 stars). We refer the interested reader to section 8 of Milone et al. (2018) for a brief discussion about some sources for material processed by p–p chain reactions that could produce the suggested He variations among P1 stars and some of their associated caveats.

Future studies with larger sample sizes are needed to explore possible correlations between Δ(F275W-F814W) and properties like [Fe/H] or $T_{\rm eff}$ that could influence the relative position of the stars along the extended P1 population of the chromosome map in a reliable manner.

## 5 SUMMARY AND CONCLUSIONS

Previous studies have been able to isolate distinct sub-populations of globular cluster stars with different light element abundances in

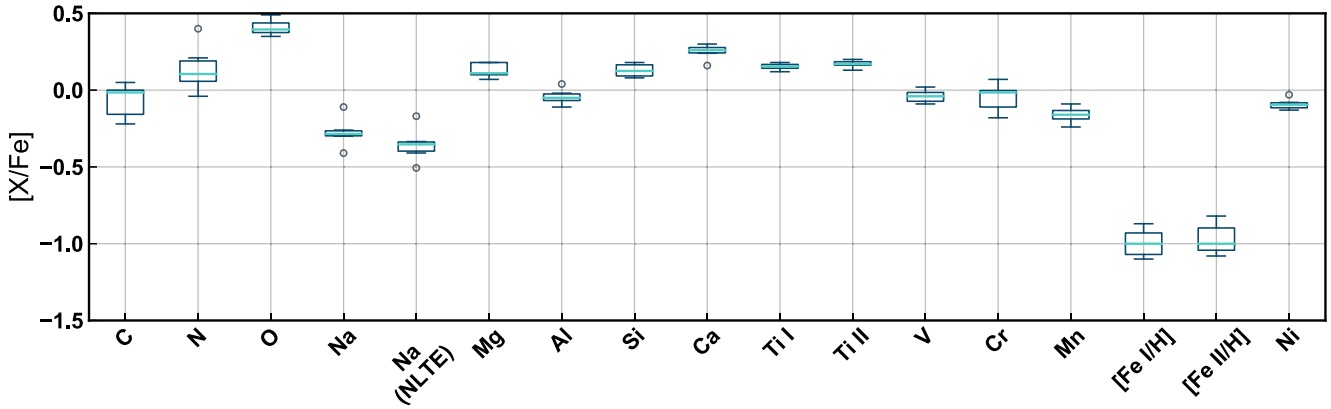


**Figure 3.** Tukey boxplot of the measured abundances of our targets. For each element, the blue box extends from the lower to upper quartile of the distribution of abundances. The cyan line in each box represents the median of the distribution, while the 'whiskers' extend to 1.5 times the value of the interquartile range, in either side of the box. Data points that lie outside the whiskers are represented with circles. From this figure one can conclude that there is no evidence for significant abundance spread among the stars of photometric groups A and B in our sample in any of these elements.

several photometric planes (e.g. Milone et al. 2015b; Carretta et al. 2018). The pseudo colour–colour plot, so-called chromosome map (a (F275W-F336W) - (F336W-F438W) versus F275W-F814W plot normalized in a convenient way) is among the most popular due to its efficacy. By modelling stellar atmospheres different groups have reached the conclusion that the vertical axis is mostly sensitive to variations in the N abundance of stars, while the horizontal axis is mostly sensitive to relative temperature changes of stars at a given magnitude, which have been speculated to be the manifestations of differences in the He mass fraction among these stars (cf. Milone et al. 2015b; Lardo et al. 2018).

According to this interpretation, the chromosome map of some clusters reveals the presence of new sub-populations of stars (the extended P1, composed of stars from group A and B in Fig. 1) which does not obey the longstanding paradigm which proposes that these populations are the consequence of abundance patterns produced by hot H-burning through the CNO-cycle. These interpretations presented independently in the works of Lardo et al. (2018) and Milone et al. (2018) suggest that C, N and O (elements processed via this nucleosynthetic channel) should remain constant among the stars of this population according to their models.

So far, only abundances of some elements (excluding N) of photometric group B stars have been reported in the literature. In this work we target stars from photometric groups A and B of NGC 2808 (a cluster with one of the largest extended P1) and analyse their abundances to test proposed interpretations of the chromosome map.

From our analysis we find that all these stars (from groups A and B) are homogeneous in C, N, O, Na, Mg and Al abundances – all products of the CNO-cycle, which are known to change significantly from star-to-star in other photometric groups – and other heavier elements, and are consistent with abundances of field stars with similar [Fe/H]. This represents a problem in the classical framework for the origin of multiple stellar populations in globular clusters, as this chemical signature is not expected and cannot be accounted in the current paradigm.

*At the moment, the presence of He variations among these stars remains speculative. However, the challenge to the old paradigm presented here does not rely on the confirmation of He spreads among these stars, but in the lack of variations in the other CNO-cycle products in stars of different photometric groups.* So, the contention for a new paradigm for GC formation and their multiple stellar populations can include now these results to the list of discrepant evidence (for other caveats see e.g. Cabrera-Ziri et al. 2015; Prantzos et al. 2017; Bastian & Lardo 2018; Carretta et al. 2018).

Having said that the confirmation of the presence or absence of He variations among the extended P1 stars could provide important clues about its origin. For example, if He variations are present in the stars with constant CNO-cycle products, one could narrow down the physical mechanisms that can produce such He enhancement to something that resembles p–p chain nucleosynthesis.

Although proper spectroscopic He studies are challenging, especially in cool stars, they are not impossible (e.g. Dupree, Strader & Smith 2011; Pasquini et al. 2011). The results presented in this letter create a strong case for these kind of observations.

## ACKNOWLEDGEMENTS

We would like to thank A. Dotter, M. Salaris, C. Johnson, C. Conroy and N. Bastian for insightful discussions and comments on an earlier version of this manuscript. Support for this work was provided by NASA through Hubble Fellowship grant HST-HF2-51387.001-A awarded by the Space Telescope Science Institute, which is operated by the Association of Universities for Research in Astronomy, Inc., for NASA, under contract NAS5-26555. CL acknowledges financial support from the Swiss National Science Foundation (Ambizione grant PZ00P2_168065).

## REFERENCES

Alonso A., Arribas S., Martínez-Roger C., 1999, A&AS, 140, 261
Alonso A., Arribas S., Martínez-Roger C., 2001, A&A, 376, 1039
Bastian N., Lardo C., 2018, ARA&A, 56, 83
Bastian N., Cabrera-Ziri I., Salaris M., 2015, MNRAS, 449, 3333
Bernstein R., Shectman S. A., Gunnels S. M., Mochnacki S., Athey A. E., 2003, Proc. SPIE, 4841, p. 1694
Bond H. E., Neff J. S., 1969, ApJ, 158, 1235
Cabrera-Ziri I. et al., 2015, MNRAS, 448, 2224
Carretta E., 2015, ApJ, 810, 148
Carretta E., Bragaglia A., Lucatello S., Gratton R. G., D'Orazi V., Sollima A., 2018, A&A, 615, A17
Cassisi S., Salaris M., 2013, Old Stellar Populations: How to Study the Fossil Record of Galaxy Formation, Wiley

Castelli F., Kurucz R. L., 2003, in Piskunov N., Weiss W. W., Gray D. F., eds, IAU Symp. Vol. 210. Modelling of Stellar Atmospheres, Astro. Soc. Pac. p. 20P
Charbonnel C., 2016, in Moraux E., Lebreton Y., Charbonnel C., eds, EAS Publications Series Vol. 80. p. 177, preprint (arXiv:1611.08855)
Dupree A. K., Strader J., Smith G. H., 2011, ApJ, 728, 155
Gratton R., Sneden C., Carretta E., 2004, ARA&A, 42, 385
Gratton R. G., Carretta E., Bragaglia A., 2012, A&AR, 20, 50
Grevesse N., Sauval A. J., 1998, Space Sci. Rev., 85, 161
Kelson D. D., 2003, PASP, 115, 688
Lardo C. et al., 2015, A&A, 573, A115
Lardo C., Salaris M., Bastian N., Mucciarelli A., Dalessandro E., Cabrera-Ziri I., 2018, A&A, 616, A168
Larsen S. S., Brodie J. P., Grundahl F., Strader J., 2014, ApJ, 797, 15
Lind K., Asplund M., Barklem P. S., Belyaev A. K., 2011, A&A, 528, A103
Marino A. F., Villanova S., Piotto G., Milone A. P., Momany Y., Bedin L. R., Medling A. M., 2008, A&A, 490, 625
Martocchia S. et al., 2018, MNRAS, 473, 2688
Milone A. P. et al., 2015a, MNRAS, 447, 927
Milone A. P. et al., 2015b, ApJ, 808, 51
Milone A. P. et al., 2017, MNRAS, 464, 3636
Milone A. P. et al., 2018, MNRAS, 481, 5098
Mucciarelli A., Pancino E., Lovisi L., Ferraro F. R., Lapenna E., 2013, ApJ, 766, 78
Mucciarelli A., Monaco L., Bonifacio P., Saviane I., 2017, A&A, 603, L7
Niederhofer F. et al., 2017, MNRAS, 464, 94
Osborn W., 1976, MNRAS, 176, 1
Pasquini L., Mauas P., Käufl H. U., Cacciari C., 2011, A&A, 531, A35
Prantzos N., Charbonnel C., Iliadis C., 2017, A&A, 608, A28
Sbordone L., Salaris M., Weiss A., Cassisi S., 2011, A&A, 534, A9
Schiavon R. P. et al., 2017a, MNRAS, 465, 501
Schiavon R. P. et al., 2017b, MNRAS, 466, 1010
Soto M. et al., 2017, AJ, 153, 19

This paper has been typeset from a TEX/LATEX file prepared by the author.